JOURNAL OF AIRCRAFT
Vol. 31, No. 6, November–December 1994

Forebody Flow Control on a Full-Scale F/A-18 Aircraft

Wendy R. Lanser* and Larry A. Meyn*
NASA Ames Research Center, Moffett Field, California 94035

A full-scale F/A-18 was tested in the 80- by 120-ft Wind Tunnel at NASA Ames Research Center to measure the effectiveness of pneumatic forebody vortex control devices. By altering the forebody vortex flow, yaw control can be maintained to angles of attack greater than 50 deg. Two forebody vortex control devices were tested: 1) a discrete circular jet and 2) a tangential blowing slot. The tests were conducted for angles of attack between 25–50 deg, and angles of sideslip from −15 to 15 deg. The Reynolds number based on wing mean aerodynamic chord ranged from 4.5 to 12.0 × 10^6. The time-averaged yawing moments, along with both time-averaged and time-dependent pressures on the forebody of the aircraft, are presented here for various configurations. Of particular interest was the result that the tangentially blowing slot had a greater effect on the yawing moment than the discrete circular jet. Additionally, it was found that blowing very close to the radome apex was not as effective as blowing slightly farther aft on the radome, and that a 16-in.-long slot was more effective than either an 8- or 48-in.-long slot.

Nomenclature

A_j = area of the discrete circular jet, 0.0055 ft^2
A_s = area of the slot, hl_s ft^2
b = reference wing span, 37.42 ft
C_p = pressure coefficient, $(p - p_\infty)/q_\infty$
Cn = body-axis yawing moment coefficient, yawing moment/$q_\infty Sb$
$C\mu$ = momentum coefficient of blowing, $\dot{m}_s V_s/q_\infty S$
h = height of blowing slot, 0.10 in.
l = length of aircraft, 54.4 ft
l_s = slot length, in.
M_∞ = freestream Mach number
MFR = mass flow ratio, $\dot{m}_s/\dot{m}_{\text{ref}}$
mac = mean aerodynamic chord, 11.52 ft
$\dot{m}_j$ = mass flow rate through the jet, $\rho_j V_j A_j$
$\dot{m}_{\text{ref}}$ = reference mass flow rate, $\rho_\infty U_\infty S$
$\dot{m}_s$ = mass flow rate through slot, $\rho_s V_s A_s$
p = static pressure, psi
p_∞ = freestream static pressure, psi
q_∞ = dynamic pressure, $\frac{1}{2}\rho_\infty U_\infty^2$
Re_c = Reynolds number based on mac
S = reference wing area, 400 ft^2
t = time, s
U_∞ = freestream velocity, ft/s
V_j = velocity at the jet exit, ft/s
V_s = velocity at the slot exit, ft/s
x = distance from nose apex along longitudinal axis of aircraft
y/s = spanwise position on the leading-edge extensions
α = angle of attack, deg
β = angle of sideslip, deg
θ = circumferential angle
ρ_s = air density at the slot exit
ρ_∞ = freestream air density
τ = convective time, tU_∞/l

Presented as Paper 92-2674 at the AIAA 10th Applied Aerodynamics Conference, Palo Alto, CA, June 22–24, 1992; received Sept. 23, 1992; revision received March 2, 1994; accepted for publication March 7, 1994.

*Aerospace Engineer. Member AIAA.

Introduction

IT has been shown experimentally that sharp-nosed, circular, slender body configurations encounter asymmetric flow separation at high angles of attack. This flow phenomenon is common to high-performance aircraft and missiles during high-angle-of-attack maneuvers.[1,2] Also, it is well known that when typical fighter aircraft operate at high angles of attack, the rudder effectiveness decreases as the vertical tails become engulfed in the wake of the forebody and the wings. At these high angles of attack the asymmetric flow separation and shed vortices on the slender forebody of the aircraft introduce significant side force on the forebody even when little or no sideslip angle is present. This induced side force results in large yawing moments on the aircraft. Flight tests and wind-tunnel measurements have shown that current aircraft at high angles of attack are unable to control these large yawing moments using conventional control surfaces. As a result, many studies have been conducted on unconventional lateral control techniques. If some mechanism is not introduced to restore the lateral control at these angles of attack, the aircraft angle-of-attack range is limited to below that desired for operational use. Some of the techniques tried in the past are forebody strakes, forward and aft blowing on the forebody through jet nozzles used independently and in conjunction with the forebody strakes, and a tangential blowing slot on the forebody.[3–11] Each of these techniques was tested at small scale in water tunnels or wind tunnels, and most were found to be effective because they modify the flowfield surrounding the forebody of the aircraft.

Of particular interest in the high-angle-of-attack program at the NASA Ames Research Center are mechanisms that use pneumatic control to improve the lateral-directional control of slender body aircraft at high angles of attack. Improved lateral control is achieved by controlling the forebody flow, which in turn provides yaw control. This article reports on the tests of a full-scale F/A-18 in the 80- by 120-ft Wind Tunnel of the National Full-Scale Aerodynamic Complex at NASA Ames Research Center as part of the NASA High Alpha Technology Program.

The primary objective of the tests reported in this article was to measure the effectiveness of pneumatic forebody vortex control in generating yawing moments at high angles of attack. This article presents the yawing moment generated with different forebody vortex control configurations and

blowing rates. Pressure measurements on the forebody are reported as both time-averaged and time-dependent quantities. Test conditions included variation in angle of attack from 25 to 50 deg, angle of sideslip from −15 to 15 deg, and freestream velocity from 67 to 168 ft/s. The Reynolds number based on wing mean aerodynamic chord ranged from 4.5 to 12.0 × 10^6. The mass flow rate of air blown through the slot varied from 0 to 1.3 lbm/s. The yawing moment used to evaluate the vortex control devices was measured using the wind-tunnel scale system. The moment reference was located at fuselage station (FS) 457.06 and water line 100, which corresponds to a c.g. at a 25% mean aerodynamic chord. The test conditions match 1 *g* flight Reynolds numbers, a fact of particular importance in forebody flow control experiments since the boundary-layer separation characteristics in the forebody region are sensitive to Reynolds number.

Description of Model

The full-scale F/A-18 aircraft tested (Fig. 1) was a single-seat aircraft built by the McDonnell Douglas Aircraft and Northrop corporations. The F/A-18 fighter aircraft has two vertical stabilizers canted 20 deg outboard from the vertical, and has leading-edge extensions (LEXs) on each side of the fuselage just forward of the wing. The instrumented LEXs used for this experiment were flown on the High Alpha Research Vehicle at Dryden Flight Research Facility in 1990.[12] During the wind-tunnel test, the aircraft had both engines removed, the wingtip missile launch racks mounted, and the control surfaces configured for high-angle-of-attack flight. The configuration for high angle of attack fixed the leading-edge flaps at 33-deg leading edge down, and the trailing-edge flaps at 0 deg. The horizontal tails were operated on a flight control schedule that was a function of angle of attack to maintain trimmed flight conditions. The rudders were positioned at 0-deg deflection unless noted otherwise.

The radome designed for these experiments incorporated two independent pneumatic vortex control mechanisms interior to the radome structure: 1) a variable length slot and 2) a discrete circular jet. The radome was a composite laminate of fiberglass/foam/fiberglass fabricated from a plastic mold formed on a production-aircraft radome. Figure 2 shows the slot and the discrete jet arrangement on the radome; only the port slot and jet were active. Care was taken to assure symmetry with the starboard side incorporating a dummy slot and jet.

The blowing slot had a total length of 48 in. and began 3 in. aft of the radome apex. The slots were positioned at 90 and 270 deg from the windward side (bottom) of the radome. The active slot was at the 270-deg position (port-side) and

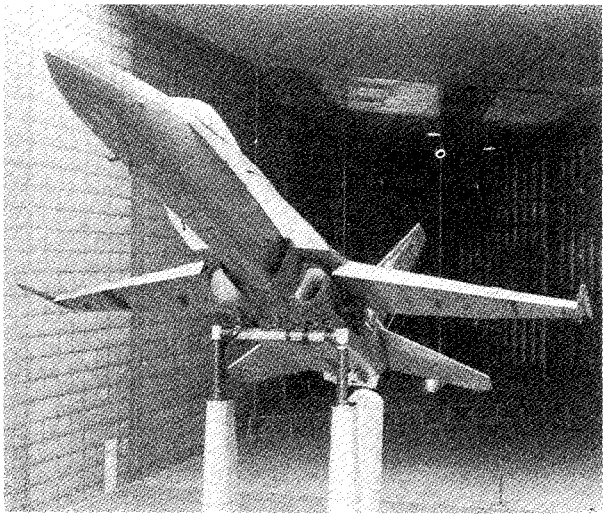

Fig. 1 F/A-18 mounted in the 80- by 120-ft Wind Tunnel test section. A three-strut configuration with mounting hardware was used.

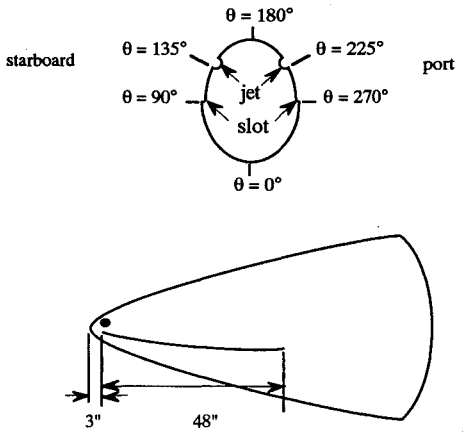

Fig. 2 Arrangement of the slot and discrete jet arrangement on the radome. The active slot and jet were located on the port side; a dummy slot and jet were on the starboard side.

was designed to blow tangential to the surface toward the leeward side of the radome. The 48-in. slot was divided into 24 separately controlled segments with each segment measuring 2 in. long. The slot height was 0.10 in.

The discrete circular jets were located 3 in. aft of the radome apex at 135 and 225 deg from the windward side and had a 1-in. exit diam. A 1-in.-diam pipe was inserted at the jet exits to obtain two additional jet configurations. The active jet was at the 225-deg position. Air for both the slot and the jet was supplied by several 125-psi compressors, totaling 1550 ft^3/min. The air passed through a plenum located in the cockpit of the aircraft, which functioned as a settling chamber before traveling to either the slot or the jet. All the hardware from the plenum to the jet and to the 2-in. slot segments were nearly identical in order to maintain a constant pressure drop across the length of the slot. The mass flow rate of the blowing air was measured with a turbine flow meter.

A three-strut configuration was used to mount the F/A-18 aircraft in the test section (Fig. 1). The aircraft was attached to a circular crossbeam at the two main landing-gear positions. The crossbeam was then attached to the wind-tunnel main struts. A tail boom assembly connected the aircraft at the pins normally used to mount the engines and the arresting tail hook normally used for aircraft carrier landings. This tail boom assembly was used to attach the aircraft to an actuator-driven tail strut. The angle of attack was varied by changing the length of the tail strut, while the sideslip angle was changed by rotating the entire balance frame. This mounting arrangement placed the crossbeam 33 ft above the floor of the test section.

Description of Experiment

Three discrete jet configurations were studied to determine the configuration that would produce the largest change in yawing moment for the minimum required blowing. To determine the optimum configuration, the position of the exhaust plane relative to the radome apex and the mass flow rate through the jet were varied. For the slot blowing, the slot position relative to the radome apex, the slot length, and the mass flow rate through the slot were varied.

To better understand the influence of the pneumatic forebody vortex control on the flowfield structure, time-averaged pressures were measured on the forebody and on each LEX. The pressure orifices were located at five fuselage stations (FS): three circumferential rings on the radome at FS 70, 85, and 107, and two circumferential rings on the forebody at FS 142 and 184 (Fig. 3). Pressure orifices were also located on both the upper and lower surfaces of the LEXs at three positions: FS 253, 296, and 357 (Fig. 3). The radome apex was located at FS 60.5 and the fuselage stations were measured in inches from that point. Each pressure orifice on the fore-

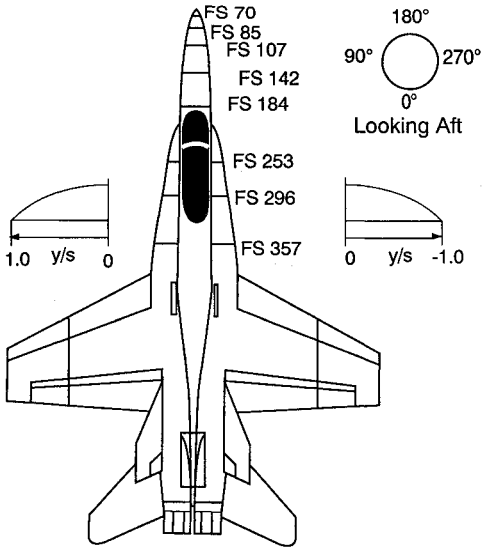

Fig. 3 Pressure orifice locations on the forebody and LEXs of the F/A-18.

body and LEXs was connected to an electronically scanned pressure transducer with 0.04-in.-o.d. tubing. The pressure orifices on the forebody were instrumented with ±2.5-psi differential-pressure transducers with accuracies of ±0.00075 psid, and the LEXs were instrumented with ±5.0-psi differential-pressure transducers with accuracies of ±0.0015 psid.

An additional parameter used to determine the effectiveness of the pneumatic forebody vortex control mechanism was the time lag or response time of the system to produce a change in the pressure throughout the local flowfield. Time-dependent pressure measurements were, therefore, taken on the forebody and LEXs. These time-dependent data were acquired at a rate of 100 samples/s for a 20-s period.

In addition to these measurements, the flowfield over the fuselage of the F/A-18 was studied using flow visualization. Smoke was introduced into the flowfield at the apex of the LEX on the port side to visualize the LEX vortex, and surface-mounted tufts were positioned on the wings and forebody showing the separation patterns on those surfaces. The smoke was used as a flow visualization tool that highlighted the LEX vortex so that it could be tracked in three dimensions with a stereo ranging system. Results from this system are available in Refs. 9 and 13.

Results

The experimental results discussed in the following section show the effectiveness of various configurations using pneumatic forebody vortex control to improve the lateral-directional control of the aircraft at high angles of attack. Data are shown for both the discrete circular jet and the tangentially blowing slot. Representative pressure distributions are presented for the blowing-off and blowing-on cases. The time delay required for the system to produce a change in the pressure throughout the local flowfield is also presented at one FS. The yawing moment data are presented in the body axes coordinate system with the change in yawing moment ΔCn defined as the difference between the blowing-off and the blowing-on measurements.

Discrete Jet Blowing

During the experiment, three port-side circular jet configurations were examined as shown in Fig. 4: 1) a jet located 3 in. aft of the radome apex blowing straight aft, 2) a jet located 16 in. aft of the apex blowing straight aft, and 3) a jet located 16 in. aft of the apex canted inward 15 deg toward the top centerline of the radome.

The aft blowing jets, 3 and 16 in. from the apex, provided significant yawing moments, particularly at $\alpha \geq 45$ deg (Fig. 4). A slightly larger moment was generated by the jet 16 in. aft of the nose than by the jet 3 in. aft of the nose at $\alpha = 45$ deg. In both cases a nose-right yawing moment was generated ($\Delta Cn > 0$). Similar results were obtained in small-scale tests of an F-16C conducted by LeMay et al.[7] The positive yawing moment means the increase in side force is due to the reduced pressure (greater suction) generated on the nonblowing side of the radome and an increase in pressure on the blowing side. The two jet configurations achieve this suction force on the nonblowing side of the radome by moving the separation location toward the windward side on the blowing side of the radome, which results in decreased pressure on the nonblowing side of the radome. The decreased pressure generates a suction force on the nonblowing side of the radome. Pressure distributions on the radome and forebody support this data. Figure 5 shows the difference in the pressure signatures between the nonblowing and maximum blowing conditions for the jet positioned at 3 in. The discontinuities in the data at $\theta = 90$ deg were caused by the dummy slot on the radome.

The jet located 16 in. aft of the radome apex and blowing inward 15 deg had the least effect on the yawing moment (Fig. 4). This jet generated a small nose-left yawing moment ($\Delta Cn \leq 0$). This yawing moment indicates that the additional side force is generated from the suction force acting on the blowing side of the radome. As a point of reference, the yawing moment generated by both rudders deflected 30 deg left is also shown in Fig. 4. The yawing moments generated by the jets located 3 and 16 in. straight aft of the radome apex were slightly more effective than the maximum rudder deflection (30 deg) at the 45- and 50-deg angle-of-attack cases.

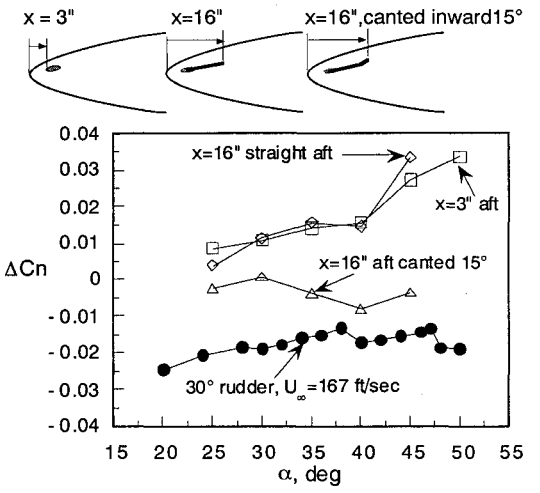

Fig. 4 Effect of angle of attack on yawing moment for three different discrete jet configurations; $U_\infty = 132$ ft/s, $\beta = 0$ deg, $MFR = 0.00022$.

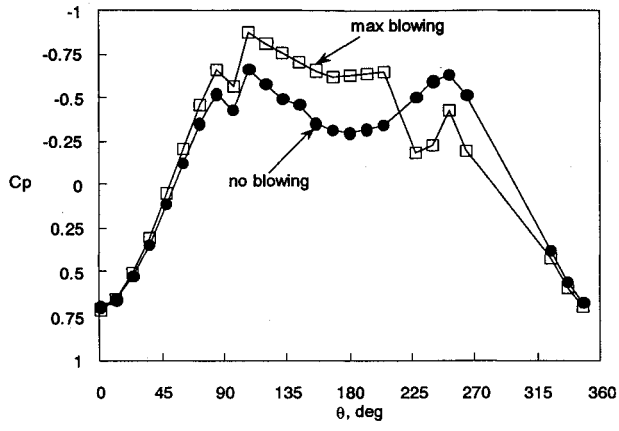

Fig. 5 Effect of discrete jet located 3 in. aft of radome apex on the pressure distribution at FS 70; $\alpha = 30$ deg, $\beta = 0$ deg, $U_\infty = 132$ ft/s.

Tangential Blowing Slot

The yawing moments generated by four slots are shown in Fig. 6. The slots were 8, 16, 32, and 48 in. long, and each began 3 in. aft of the radome apex. The *MFR* through each of the slots varied with slot length; at the conditions shown in Fig. 6, the 32- and 48-in.-long slots had the largest effect on the yawing moment throughout the entire angle-of-attack range.

The position of the slot relative to the radome apex also had an effect on the amount of side force generated. The various slot positions relative to the radome apex are shown in Fig. 7. Figure 8a shows that for an *MFR* of 0.00026, the 16-in. slot positioned at 3 in. was not as effective as when positioned 11 or 19 in. aft of the radome apex. Note that the 16-in. slot positioned at 11 or 19 in. produced nearly the same moments as the 32- or the 48-in. slots positioned at 3 in. (Fig. 6) for a lower mass flow rate. For comparison, the change in yawing moments due to 30 deg of left rudder deflection are shown in Figs. 8a and 8b. It is clear that slot blowing produced much larger moments than the maximum rudder deflection at angles of attack greater than 30 deg.

Figure 8b shows data for the same mass flow rate as in Fig. 8a; however, the freestream velocity was increased yielding a lower *MFR*. For the lower *MFR*, the 16-in. slot positioned 11 and 19 in. aft of the radome apex again proved to be more effective than when positioned 3 in. aft of the radome apex. The tangential slot blowing produced a side force in the direction of the blowing side of the radome. This result indicates that the tangential slot blowing keeps the flow attached along the blowing side of the radome. This flow phenomenon, called the coanda effect, creates a low pressure on the blowing side of the radome, resulting in a suction force. Thus, blowing from the left side of the radome will produce a nose-left yawing moment. It was also noticed that blowing 11 or 19 in. aft of the apex allows this low pressure to affect more surface area, resulting in a greater yawing moment than for 3 in. aft of the apex. Also, the tighter radius very near the nose of the radome could defeat the coanda effect.

Based on the results presented above, the 16- and 32-in. slots beginning 11 in. aft of the radome apex were the most

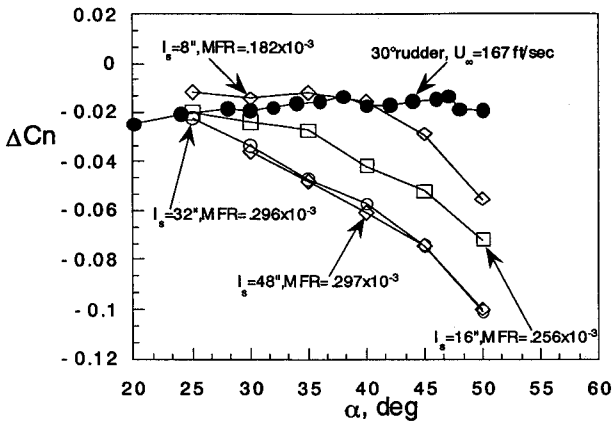

Fig. 6 Variation of yawing moment with angle of attack and slot length. Each slot began 3 in. aft of the radome apex; β = 0 deg, U_∞ = 132 ft/s.

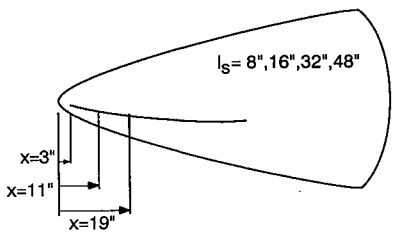

Fig. 7 Schematic of the various slot positions relative to the radome apex.

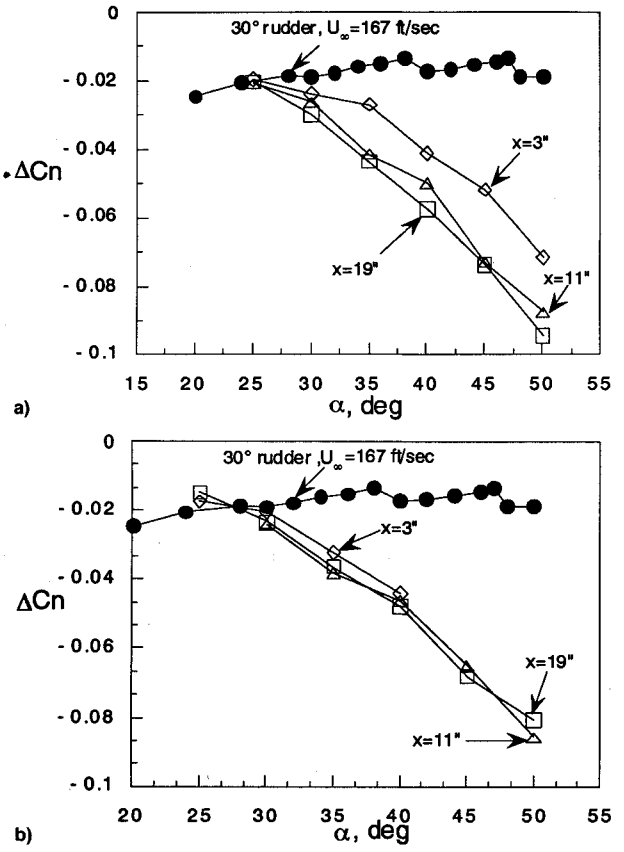

Fig. 8 Effect of angle of attack on yawing moment for various slot positions on the radome; l_s = 16 in., β = 0 deg: a) U_∞ = 132 ft/s, *MFR* = 0.00026 and b) U_∞ = 167 ft/s, *MFR* = 0.00022.

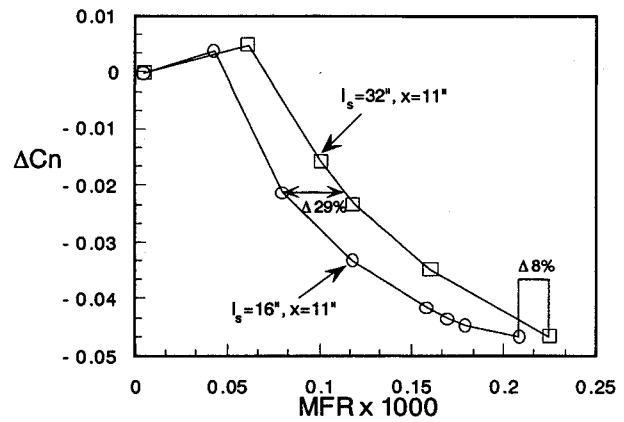

Fig. 9 Effect of mass flow ratio on yawing moment; α = 40 deg, β = 0 deg, U_∞ = 168 ft/s.

effective; consequently, they were tested over an expanded range of mass flow rates. For a given yawing moment, the 16-in. slot used between 8–30% less mass flow than did the 32-in. slot (Fig. 9). Both the 16- and 32-in. slots produced a small moment reversal at very low mass flow ratios. This moment reversal also appeared in the water-tunnel experiments of slot blowing on the forebody of a fighter aircraft.[5] This result may be related to results presented by Ericsson,[14] which showed side force reversals for a rotating circular cylinder at low rotation speeds.

Figure 10 shows the relationship between the blowing momentum coefficient $C\mu$ and the *MFR* for four slot lengths. The data shown in Fig. 10 include freestream velocities of 132 and 168 ft/s. In these experiments, the exit velocities through the slots ranged from subsonic to sonic flow as the mass flow through the slots was increased. The 48- and 32-in. slots maintained subsonic flow conditions throughout the range of mass

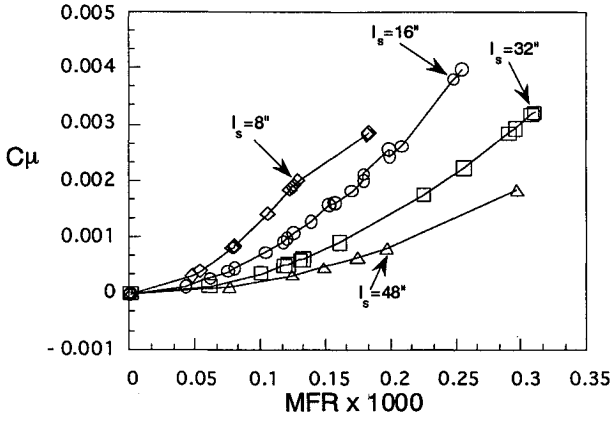

Fig. 10 Effect of the mass flow ratio on the blowing momentum coefficient for various slot lengths.

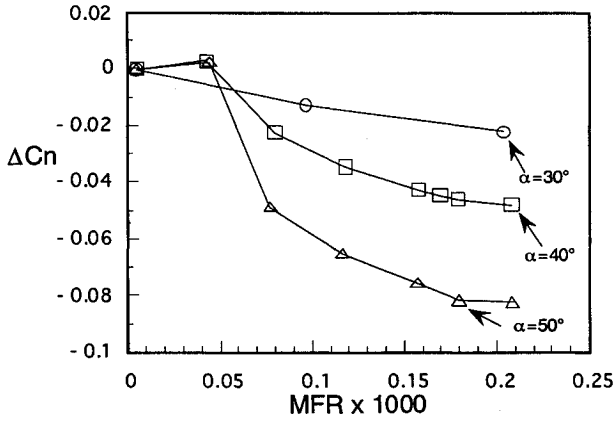

Fig. 11 Effect of the mass flow ratio on yawing moment for various angles of attack; l_s = 16 in., x = 11 in., β = 0 deg, U_∞ = 168 ft/s.

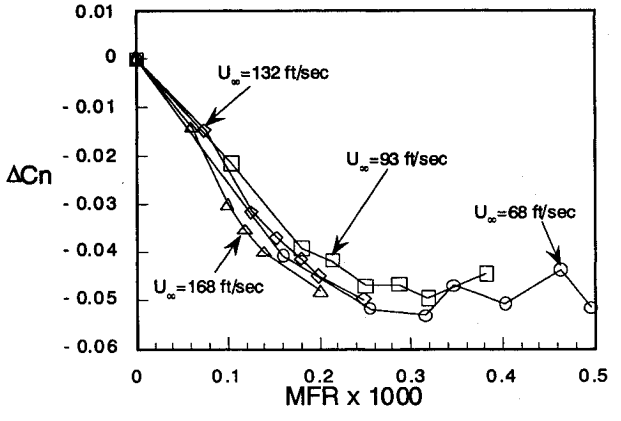

Fig. 12 Effect of the mass flow ratio on yawing moment for various freestream velocities; l_s = 16 in., x = 11 in., α = 40 deg, β = 0 deg.

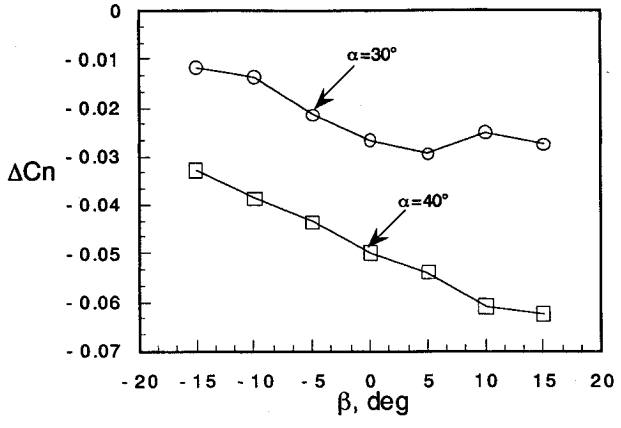

Fig. 13 Effect of sideslip angle on yawing moment for 30- and 40-deg angles of attack; l_s = 16 in., x = 11 in., β = 0 deg, U_∞ = 132 ft/s, MFR = 0.00026.

flow rates tested. The 16-in. slot had sonic flow conditions at an MFR of 0.0002 for a U_∞ of 168 ft/s, and at an MFR of 0.0025 for a U_∞ of 132 ft/s. For the 8-in. slot, sonic flow conditions occurred at an MFR of 0.00013 for a U_∞ of 132 ft/s. The data show that the 8-in. slot reached sonic conditions for a lower MFR than the other slot configurations. This may explain the difference in the shape of the MFR vs $C\mu$ curve for the 8-in. slot when compared to the 16-, 32-, or 48-in. slots.

The measured mass flow rate, plenum temperature, slot exit area, and wind-tunnel static pressure were used to determine the slot exit conditions. The exit Mach number, velocity, and $C\mu$ were determined using the continuity relationship defined in Ref. 15. This relationship assumed a uniform exit velocity.

Tangential slot blowing proved to be effective across the entire angle-of-attack range; in fact, its effectiveness increased as the angle of attack was increased (Fig. 11). The results indicate a small moment reversal at very low mass flow rates for the 40- and 50-deg angle-of-attack cases. Data were not taken for small mass flows at α = 30 deg.

The effect of Reynolds number was also examined in the tunnel by testing various velocities up to the maximum of 168 ft/s. Figure 12 shows the variation of yawing moment with MFR for the 16-in. slot, 11 in. aft of the apex, and at α = 40 deg. Results are shown for various wind-tunnel velocities; there is little difference between the curves. These results indicate that slot blowing was not sensitive to Reynolds number across this range of velocities. Additionally, trip strips were used to simulate the boundary-layer transition on the radome at higher Reynolds numbers. Serrated edge tape (0.015 in. thick) was applied to the radome at 45 and 315 deg in an effort to fix the boundary-layer transition. There was no significant change in the yawing moment produced by the forebody blowing from the trip-strip-on and trip-strip-off configurations.

The tangential slot blowing also proved to be effective in providing lateral-directional control of the aircraft at sideslip angles from −15 to 15 deg (Fig. 13). Similar to the zero sideslip results discussed previously, slot blowing is more effective at α = 40 deg than at α = 30 deg over the sideslip range tested. These data demonstrate that the slot blowing on a given side can generate significant yawing moments when the aircraft is yawed in either direction. For example, if the aircraft had a natural tendency to yaw to the right ($-\beta$), blowing on the left side of the radome could still generate a net nose left ($+\beta$) yawing moment.

Some of the flow mechanisms at work in slot blowing can be discerned by examining the pressure distributions on the forebody. In the following discussion of pressure distributions, surface flow visualization photographs from the High Alpha Research Vehicle (HARV)[12] were used to aid in the interpretation of the results. The HARV surface flow visualization photographs used were at 47-deg angle of attack, 0-deg sideslip, and 1 g steady-state flight. Figure 14a is an illustration of the forebody crossflow behavior observed during the current tests for the blowing-off and blowing-on cases. The tangential slot blowing keeps the flow attached along the blowing side of the radome. This flow phenomenon (the coanda effect) creates a low pressure on the blowing side of the radome, resulting in a suction force and, thus, a yawing moment. The pressure distributions for forebody FS 70–142 and LEX FS 253 and 357 are presented in Figs. 14b–14f. At FS 70 (Fig. 14b) there was little difference between the blowing-off and the blowing-on condition, because this section was approximately 1 in. forward of where the slot began. Evidence of a vortex signature on either side of the radome was seen at θ of 155 and 204 deg.

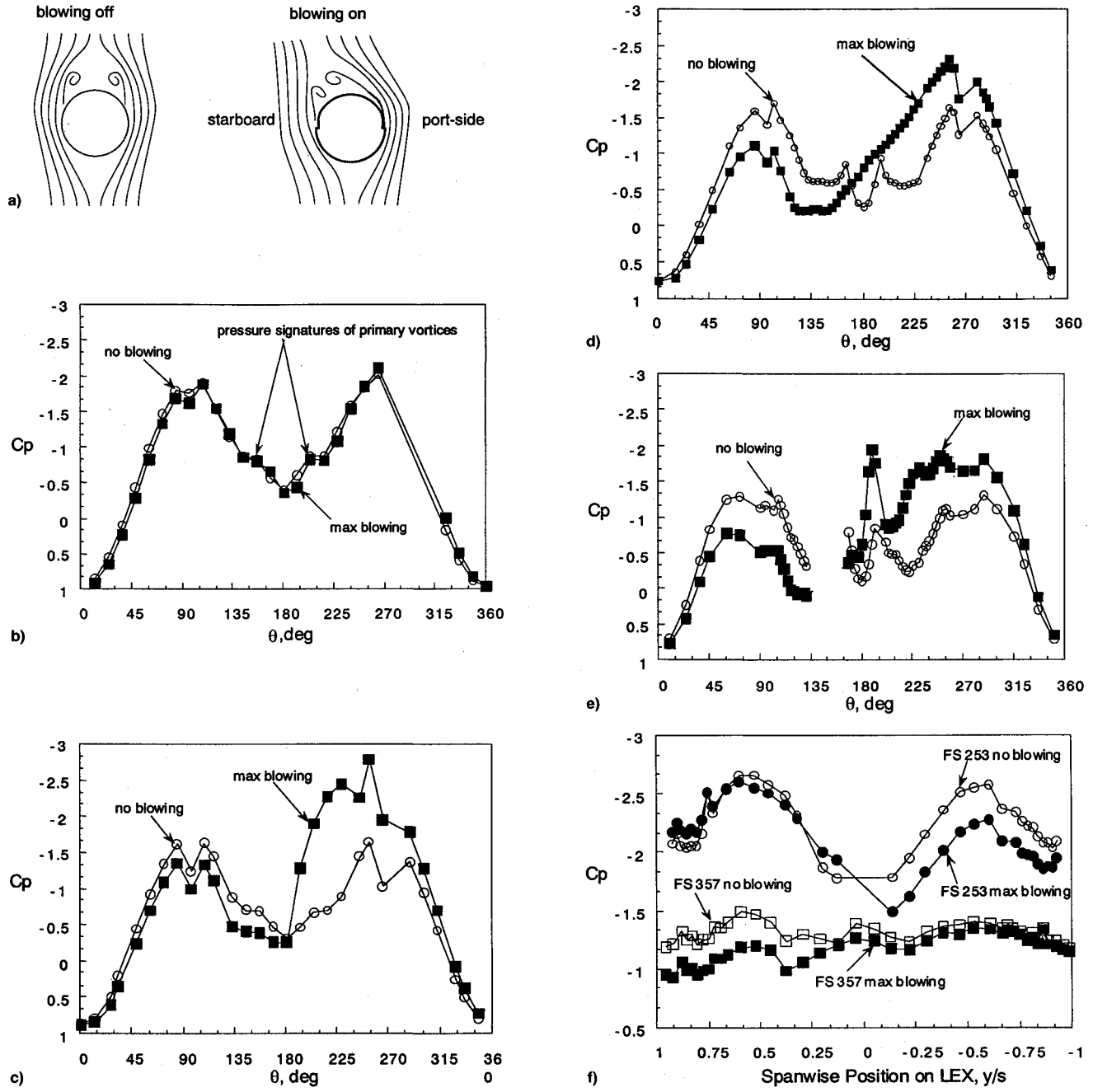

Fig. 14 Forebody and LEX pressure distributions for the 16-in. slot located 11 in. aft of the apex; α = 50 deg, β = 0 deg, U_∞ = 167 ft/s: a) sketch of flow behavior for the blowing-off and blowing-on cases on a circular forebody, b) FS 70, c) FS 85, d) FS 107, e) FS 142, and f) FS 253 and FS 357.

Similar to FS 70, the no-blowing case at FS 85 showed evidence of a vortex signature on either side of the radome at θ of 155 and 204 deg (Fig. 14c). However, for the blowing-on case, no conclusive vortex signature was seen on the blowing side of the radome. A vortex may be present on the nonblowing side of the radome at θ of 155 deg, but it is difficult to conclude this effect of blowing without corresponding flow visualization. The discontinuities in the data at θ of 96 and 264 deg for the no-blowing case, and at θ of 96 and 264 deg for the blowing-on case, are due to the geometry variations at the slot.

At FS 107 (Fig. 14d) the no-blowing case shows a vortex signature on either side of the radome at θ of 165 and 195 deg. These suction peaks are very close to the secondary separation lines visualized during F-18 HARV flight tests.[12] For the blowing-on case, the pressure decreased on the blowing-side of the radome while the pressure on the nonblowing side increased. The reattachment point also moved toward the no-blowing side of the radome. Again, the discontinuities in the data at the θ of 96 and 264 deg for both the no-blowing and blowing-on cases are due to the geometry variations at the slot.

At FS 142 (Fig. 14e) the nonblowing case showed a vortex signature at θ = 195 deg on the blowing side, and near θ = 170 deg on the no-blowing side. For the blowing-on case, a strong vortex signature appears at θ = 195 deg. This differs from FS 107 where no vortex signature was present on either side of the radome with blowing activated. Unfortunately, pressure taps could not be located at 131 deg < θ < 167 deg due to structural obstructions inside the aircraft.

In the LEX upper surface pressure distributions for FS 253 and FS 357 (Fig. 14f), the no-blowing cases appear to be asymmetric. The blowing-on case for FS 253 showed an increased pressure on the blowing side, which is the reverse of what was seen on the forebody pressures. The LEX pressures on the nonblowing side also showed opposite behavior from

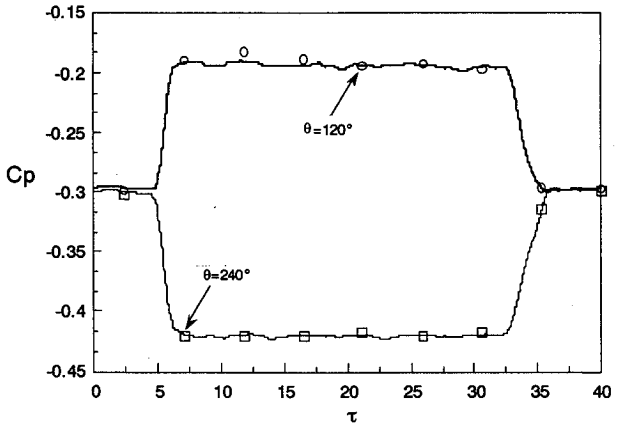

Fig. 15 Pressure time history for the pneumatic forebody flow control system to influence the flowfield; FS 107, l_s = 16 in., x = 11 in., α = 50 deg, β = 0 deg, U_∞ = 132 ft/s.

the forebody pressures with decreased pressures in the spanwise regions between 0.14–0.20 and 0.73–0.93. At FS 357, when the no-blowing case is compared to the blowing-on case, the data show a gradual increase in pressure from the blowing side of the aircraft to the nonblowing side of the aircraft. These data may indicate that the tangential slot blowing influences the interaction of the forebody and LEX vortices over the canopy region of the aircraft.

Time Lag

Knowledge of the time required for the pneumatic forebody flow control system to produce a steady-state yawing moment is important if this mechanism is to be used in flight. During the wind-tunnel experiments, unsteady pressures were measured at several points along the forebody while the blowing was turned on. Figure 15 shows the pressure coefficient as a function of τ for the 16-in. slot located 11 in. aft of the radome apex at FS 107 and θ = 240 deg (blowing side) and θ = 120 deg (nonblowing side). Blowing was activated at τ = 2.5 and turned off at τ = 30.5. For the pressures to read a steady-state value when blowing was activated τ = 5; when blowing was turned off τ = 6.5. The symbols shown represent every 200th point acquired. This data indicated that the full yawing moment developed within τ = 5.0, thus the aircraft traveled less than five body lengths before the full moment developed.

Conclusions

The primary objective of the research reported in this article was to measure the effectiveness of pneumatic forebody vortex control mechanisms in generating lateral-directional control of the F/A-18 at high angles of attack. The two discrete circular jet configurations blowing straight aft showed a measurable effect on the yawing moment, whereas the jet configuration canted 15 deg inward toward the top dead centerline of the radome had no significant effect on the yawing moment. The discrete jets tested produced slightly larger moments than the maximum rudder deflection above 40-deg angle of attack; therefore, additional work is necessary to improve the performance of these jet configurations. The tangential slot blowing was effective in providing the desired yawing moment for lateral-directional control at high angles of attack. Blowing 11 in. aft of the radome apex was more effective than blowing 3 in. aft. Also, the 16- and 32-in.-long slots were more effective and efficient than either the 8- or 48-in.-long slots. Additionally, the full-scale results showed that the effect of the tangential slot blowing on the yawing moment increased with the angle of attack, the angle of sideslip, and the mass flow of air blowing through the slot.

The time-averaged pressure distributions measured during the wind-tunnel experiments were consistent with the time-averaged force and moment data. The tangential slot blowing created a low pressure on the blowing side of the radome, keeping the flow attached on the blown side and increasing the pressure on the nonblown side, resulting in a reduced pressure force. Thus, blowing from the left-side of the radome produced a nose-left yawing moment. Tangential slot blowing increased the pressure on the forward LEX position corresponding to the blown side of the radome, and the aft LEX position showed an increased pressure along both LEXs.

At FS 107 the convective time for the pressures to read steady-state values for turning the blowing on was 5.0, whereas, for turning the blowing off it was 6.5. These results are important for the design of a flight control system because compensation must be made to allow for the difference in the response time from turning the blowing system on and off.

References

[1]Ericsson, L. E., "Flow Unsteadiness Considerations in High-Alpha Testing," *Journal of Aircraft*, Vol. 25, No. 11, 1988, pp. 1033–1037.

[2]Ericsson, L. E., and Reding, J. P., "Dynamics of Forebody Flow Separation and Associated Vortices," *Journal of Aircraft*, Vol. 22, No. 4, 1985, pp. 329–335.

[3]Malcolm, G. N., and Ng, T. T., "Forebody Vortex Manipulation for Aerodynamic Control of Aircraft at High Angles of Attack," Society of Automotive Engineers Paper 892220, Sept. 1989.

[4]Malcolm, G. N., Ng, T. T., Lewis, L. C., and Murri, D. G., "Development of Nonconventional Control Methods for High Angle of Attack Flight Using Vortex Manipulation," AIAA Paper 89-2192, Aug. 1989.

[5]Ng, T., Suarez, C., and Malcolm, G., "Forebody Vortex Control Using Slot Blowing," AIAA Paper 91-3254, Sept. 1991.

[6]Guyton, R. W., and Maerki, G., "X-29 Forebody Jet Blowing," AIAA Paper 92-0017, Jan. 1992.

[7]LeMay, S. P., Sewall, W., and Henderson, J., "Forebody Vortex Flow Control on the F-16C Using Tangential Slot and Jet Nozzle Blowing," AIAA Paper 92-0019, Jan. 1992.

[8]Gee, K., Tavella, D., and Schiff, L. B., "Computational Optimization of a Pneumatic Fuselage Forebody Flow Control Concept," AIAA Paper 91-3249, Sept. 1991.

[9]Meyn, L. A., Lanser, W. R., and James, K. D., "Full Scale High Angle of Attack Tests of an F/A-18," AIAA Paper 92-2676, June 1992.

[10]Gee, K., Rizk, Y. M., Murman, S. M., Lanser, W. R., Meyn, L. A., and Schiff, L. B., "Analysis of a Pneumatic Forebody Flow Control Concept About a Full Aircraft Geometry," AIAA Paper 92-2678, June 1992.

[11]Lanser, W. R., and Murri, D. G., "Wind Tunnel Measurements on a Full-Scale F/A-18 with Forebody Slot Blowing or Forebody Strakes," AIAA Paper 93-1018, Feb. 1993.

[12]Fisher, D., Banks, D., and Richwine, D. M., "F-18 High Alpha Research Vehicle Surface Pressures: Initial In-Flight Results and Correlation with Flow Visualization and Wind-Tunnel Data," AIAA Paper 90-3018, Aug. 1990.

[13]Meyn, L. A., and Bennett, M. S., "Application of a Two Camera Video Imaging System to Three-Dimension Vortex Tracking in the 80- by 120-Foot Wind Tunnel," AIAA Paper 93-3439, Aug. 1993.

[14]Ericsson, L. E., "Moving Wall Effects in Unsteady Flow," *Journal of Aircraft*, Vol. 25, No. 11, 1988, pp. 977–990.

[15]Society of Automotive Engineers, Inc., "Thermodynamics of Incompressible and Compressible Fluid Flow," Aerospace Information Rept., AIR1168/1, March 1990, pp. 85–87.